The Calcium-Sensing Receptor Promotes Urinary Acidification to Prevent Nephrolithiasis

Kirsten Y. Renkema,* Ana Velic,† Henry B. Dijkman,‡ Sjoerd Verkaart,* Annemiete W. van der Kemp,* Marta Nowik,† Kim Timmermans,* Alain Doucet,§ Carsten A. Wagner,† René J. Bindels,* and Joost G. Hoenderop*

*Department of Physiology, Nijmegen Centre for Molecular Life Sciences, and ‡Department of Pathology, Radboud University Nijmegen Medical Centre, Nijmegen, Netherlands; †Institute of Physiology and Zürich Center for Integrative Human Physiology, University of Zurich, Zurich, Switzerland; and §Laboratoire de Physiologie et Génomique Rénales, CNRS/UPMC UMR 7134, Institut des Cordeliers, Paris, France

ABSTRACT

Hypercalciuria increases the risk for urolithiasis, but renal adaptive mechanisms reduce this risk. For example, transient receptor potential vanilloid 5 knockout (TPRV5$^{-/-}$) mice lack kidney stones despite urinary calcium (Ca^{2+}) wasting and hyperphosphaturia, perhaps as a result of their significant polyuria and urinary acidification. Here, we investigated the mechanisms linking hypercalciuria with these adaptive mechanisms. Exposure of dissected mouse outer medullary collecting ducts to high (5.0 mM) extracellular Ca^{2+} stimulated H^+-ATPase activity. In TRPV5$^{-/-}$ mice, activation of the renal Ca^{2+}-sensing receptor promoted H^+-ATPase–mediated H^+ excretion and downregulation of aquaporin 2, leading to urinary acidification and polyuria, respectively. Gene ablation of the collecting duct-specific B1 subunit of H^+-ATPase in TRPV5$^{-/-}$ mice abolished the enhanced urinary acidification, which resulted in severe tubular precipitations of Ca^{2+}-phosphate in the renal medulla. In conclusion, activation of Ca^{2+}-sensing receptor by increased luminal Ca^{2+} leads to urinary acidification and polyuria. These beneficial adaptations facilitate the excretion of large amounts of soluble Ca^{2+}, which is crucial to prevent the formation of kidney stones.

J Am Soc Nephrol 20: 1705–1713, 2009. doi: 10.1681/ASN.2008111195

Hypercalciuria constitutes the main risk factor in urolithiasis. Patients with renal stone disease experience severe pain, a high rate of recurrence, slowly progressing tissue damage, and eventually renal insufficiency, and recurrent clinical treatment is needed.[1,2] Different types of hypercalciuria are known. In this respect, absorptive, renal, and resorptive hypercalciuria are distinguished: Disturbed intestinal Ca^{2+} hyperabsorption, impaired renal Ca^{2+} reabsorption, and increased bone resorption, respectively, are primarily involved.[3–6] Current treatment strategies of renal stones consist of (pain) medication, dietary adjustments, hydration, extracorporeal shock wave treatment, or surgery.

The transient receptor potential vanilloid member 5 (TRPV5), the epithelial Ca^{2+} channel, which is expressed in the renal distal convoluted tubule (DCT) and the connecting tubule (CNT), constitutes the major apical entry step of Ca^{2+} from the pro-urine into the renal cells.[7] TRPV5 knockout (TRPV5$^{-/-}$) mice demonstrate a robust hypercalciuria with hyperphosphaturia, predisposing these mice to an increased risk for renal Ca^{2+}-phosphate stone formation.[8] Concomitantly, TRPV5$^{-/-}$ mice display profound polyuria and increased urinary

Received November 21, 2008. Accepted March 10, 2009.

Published online ahead of print. Publication date available at www.jasn.org.

Correspondence: Dr. Joost G. Hoenderop, Physiology 286, Radboud University Nijmegen Medical Centre, P.O. Box 9101, NL-6500 HB Nijmegen, Netherlands. Phone: +31-24-3610580; Fax: +31-24-3616413; E-mail: j.hoenderop@ncmls.ru.nl

acidification.[8] Urinary acidification occurs along different segments of the nephron and is of crucial importance in acid/base homeostasis.[9,10]

In combination with urinary buffers, the activity of acid/base transporters in intercalated cells (ICs) of CNT and collecting duct system (CD) accomplish the fine-tuning of urinary pH. In type A ICs, the multisubunit vacuolar ATP-driven proton pump (H^+-ATPase) is expressed at the apical membrane, which is mainly responsible for proton excretion.[11] Inactivating mutations in the genes encoding individual subunits of the H^+-ATPase proton pump are associated with distal renal tubular acidosis, characterized by a decrease in net proton secretion.[12–14] The formation of less acidic urine predisposes to urolithiasis as the crystallization of Ca^{2+}-phosphate occurs *via* the conversion of phosphate to its divalent form (HPO_4^{2-}) in an alkaline rather than in an acidic environment.[15,16] Previously, insufficient urinary acidification was demonstrated in recurrent stone formers.[17,18] Currently, no clinical trials have documented the description of the prevention of stone formation by stimulating urinary acidification.

Aquaporin 2 (AQP2) is the water channel localized at the apical membrane of the CNT and CD that is responsible for vasopressin-regulated urinary water reabsorption.[19,20] Previous studies linked Ca^{2+} and water homeostasis, suggesting a functional role for the G-protein–coupled Ca^{2+}/polyvalent cation-sensing receptor (CaSR).[21–23] Immunolocalization studies of renal CaSR in rats revealed expression on the apical membrane of both proximal tubule and CD, the basolateral membrane of thick ascending limb of Henle (TAL), and a dif-

Table 1. Physiologic parameters of control and TRPV5$^{-/-}$ mice[a]

Parameter	Control	TRPV5$^{-/-}$
Urine		
Ca^{2+} (μmol/24 h)	10 ± 2	132 ± 31[b]
phosphate (μmol/24 h)	65 ± 8	142 ± 13[b]
citrate (mg/24 h)	40 ± 10	56 ± 13
oxalate (μmol/24 h)	3.4 ± 0.9	2.7 ± 0.5
volume (ml/24 h)	1.5 ± 0.3	3.6 ± 0.5[b]
pH	7.4 ± 0.1	5.5 ± 0.1[b]
osmolality (mOsmol/kg)	1928 ± 201	1222 ± 175[b]
Serum		
Ca^{2+} (mM)	2.36 ± 0.02	2.42 ± 0.02
ionized Ca^{2+} (mM)	1.27 ± 0.01	1.30 ± 0.01
phosphate (mM)	2.5 ± 0.2	2.3 ± 0.1

[a]Urine and serum biochemical parameters of 8-wk-old control and TRPV5$^{-/-}$ mice. Data are means ± SEM (n = 5).
[b]$P < 0.05$, significant difference from control mice.

Table 2. Urinary TA in control and TRPV5$^{-/-}$ mice[a]

Parameter	Control	TRPV5$^{-/-}$
NH_3/NH_4^+ (mmol/24 h)	0.033 ± 0.006	0.036 ± 0.007
TA (mEq/24 h)	0.048 ± 0.007	0.121 ± 0.006[b]
HCO_3^- (mmol/24 h)	0.002 ± 0.001	0.001 ± 0.001
NAE (mEq/24 h)	0.083 ± 0.012	0.157 ± 0.012[b]
pH	6.2 ± 0.1	5.6 ± 0.1[b]

[a]Urinary TA in a novel experiment with 8-wk-old control and TRPV5$^{-/-}$ mice (n = 7). Data are means ± SEM.
[b]$P < 0.001$, significant difference from control mice.

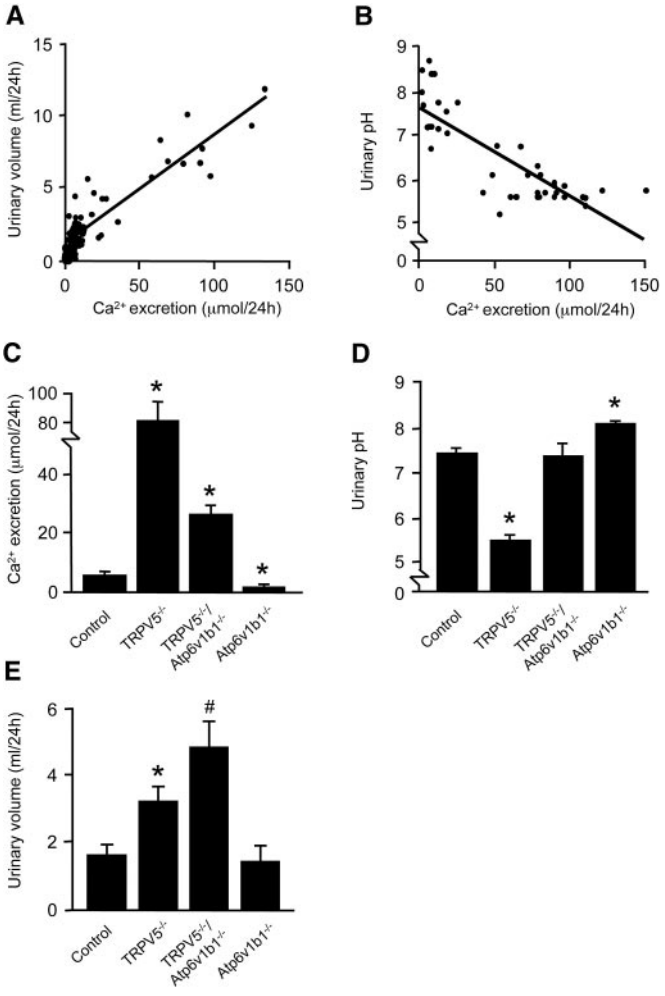

Figure 1. Urinary Ca^{2+} excretion, volume, and pH. (A and B) Correlation of urinary Ca^{2+} excretion with (A) urinary volume and (B) urinary pH in control and TRPV5$^{-/-}$ mice. Each dot represents single mouse datum. Linear regression analysis confirmed significant correlations of urinary Ca^{2+} excretion with urinary volume (r^2 = 0.83; $P < 0.0001$; n = 62) and urinary pH (r^2 = 0.70; $P < 0.0001$; n = 42). (C) Urinary Ca^{2+} excretion was determined in 24-h urine samples of 5-wk-old control, TRPV5$^{-/-}$, TRPV5$^{-/-}$/Atp6v1b1$^{-/-}$, and Atp6v1b1$^{-/-}$ mice. TRPV5$^{-/-}$ and TRPV5$^{-/-}$/Atp6v1b1$^{-/-}$ mice showed a significant hypercalciuria, whereas hypocalciuria was present in Atp6v1b1$^{-/-}$ mice compared with control mice. (D) TRPV5$^{-/-}$ mice demonstrated a significant decrease in urinary pH compared with control mice, whereas TRPV5$^{-/-}$/Atp6v1b1$^{-/-}$ mice exhibited urinary pH levels similar to controls. Impaired urinary acidification in Atp6v1b1$^{-/-}$ mice resulted in an increase of urinary pH. (E) An increased urinary volume was demonstrated in TRPV5$^{-/-}$ compared with control mice. TRPV5$^{-/-}$/Atp6v1b1$^{-/-}$ mice displayed a further increase in 24-h urinary volume compared with TRPV5$^{-/-}$ mice. In C through E, data are means ± SEM. *$P < 0.05$ (n = 6; significant difference from control); #$P < 0.05$ (n = 6; significant difference from TRPV5$^{-/-}$ mice).

fuse pattern throughout the DCT.[24] Renal CaSR expression is highest in TAL cells and is absent from the glomerulus. The differential expression and localization of CaSR along the nephron is indicative of the variety of physiologic functions throughout the kidney. The localization of the CaSR along the CD facilitates the activation of the receptor during a hypercalciuric state.[24] In the CD, a CaSR-mediated decrease of the urine concentrating ability could eventually lead to polyuria, assisting the excretion of large amounts of Ca^{2+}.[23]

The aim of this study was to elucidate molecular mechanisms involved in the adaptations that prevent renal stone formation during hypercalciuria. The TRPV5$^{-/-}$ mouse model was used because polyuria and increased urinary acidification naturally occur in these hypercalciuric mice. The crucial roles of the functional H^+-ATPase proton pump, the AQP2 water channel, and the CaSR are demonstrated in these hypercalciuria-related adaptations. This study provides new insights regarding the formation and prevention of kidney stones.

RESULTS

Metabolic Studies

At 8-wk-old TRPV5$^{-/-}$ and littermate control mice were housed in metabolic cages for 24 h and killed. Genetic ablation of TRPV5 resulted in hypercalciuria, and these mice remained normocalcemic (Table 1). In addition, TRPV5$^{-/-}$ mice displayed hyperphosphaturia with normal serum phosphate levels and a significant polyuria with decreased urinary osmolality. Urinary citrate and oxalate excretion levels were not different between the two mouse strains. Urinary pH was significantly lower in TRPV5$^{-/-}$ mice compared with control mice. The 24-h ammonium and HCO_3^- excretion levels were unchanged (Table 2). Furthermore, urinary titratable acidity (TA) was significantly increased in TRPV5$^{-/-}$ mice. Consequently, renal net acid excretion (NAE), which is the sum of renal ammonium excretion and TA minus HCO_3^- excretion, was elevated in TRPV5$^{-/-}$ mice. Ca^{2+} excretion levels correlated linearly with urinary volume as well as pH (Figure 1, A and B, respectively). To address the contribution of H^+-ATPase activity to the acidified urine in TRPV5$^{-/-}$ mice, we generated TRPV5$^{-/-}$/Atp6v1b1$^{-/-}$ mice that were genetically ablated for both TRPV5 and the IC-specific B1 subunit of H^+-ATPase (Atp6v1b1). Hypercalciuria remained present in 5-wk-old TRPV5$^{-/-}$/ATP6v1b1$^{-/-}$ mice, although less than in TRPV5$^{-/-}$ mice (Figure 1C). Urinary pH was normalized (Figure 1D) whereas urinary volume was further increased in TRPV5$^{-/-}$/ATP6v1b1$^{-/-}$ mice in comparison with TRPV5$^{-/-}$ mice (Figure 1E).

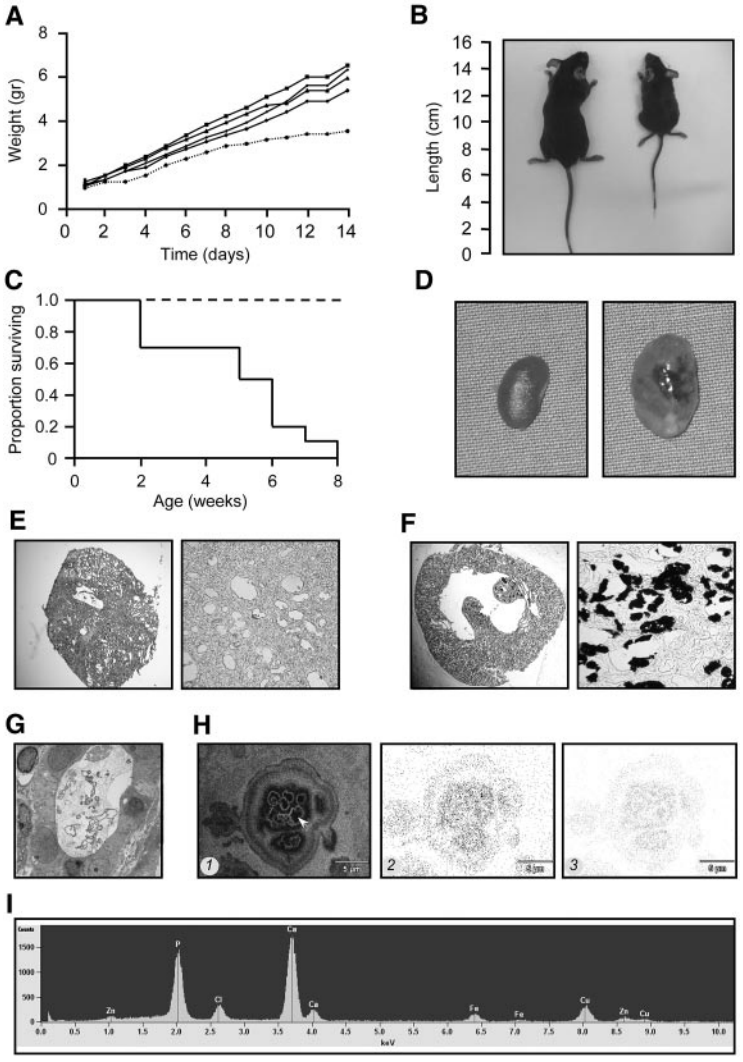

Figure 2. Analysis of TRPV5$^{-/-}$/Atp6v1b1$^{-/-}$ mice. (A) Growth curves comparing body weights of mouse genotypes, representing a litter containing one TRPV5$^{-/-}$/Atp6v1b1$^{-/-}$ mouse that died at 14 d of age (dotted line) and four littermates (solid lines). (B) Growth retardation in TRPV5$^{-/-}$/Atp6v1b1$^{-/-}$ mice, demonstrating 5-wk-old control (left) and TRPV5$^{-/-}$/Atp6v1b1$^{-/-}$ (right) mice. (C) Mortality rate of TRPV5$^{-/-}$/Atp6v1b1$^{-/-}$ (solid line; $n = 10$) and littermate (dotted line; $n = 55$) mice. (D) Kidneys from 5-wk-old control (left) and TRPV5$^{-/-}$/Atp6v1b1$^{-/-}$ mice (right). (E) Renal histology of a 5-wk-old TRPV5$^{-/-}$/Atp6v1b1$^{-/-}$ mouse. (F) Von Kossa staining in renal sections of a 1-wk-old TRPV5$^{-/-}$/Atp6v1b1$^{-/-}$ mouse. (G) Transmission electron microscopy image of a tubular precipitate in the medullary collecting duct of a 1-wk-old TRPV5$^{-/-}$/Atp6v1b1$^{-/-}$ mouse. (H) STEM image of (*1*) a precipitate, x-ray maps separately depicting (*2*) Ca^{2+}, and (*3*) phosphorus content. (I) Energy dispersive x-ray microanalysis of the renal precipitate (arrow in H) demonstrating Ca^{2+} and phosphorus content. This spectrum represents all spot measurements performed ($n = 35$ spots). Magnifications: ×100 in E (left), F (left); ×250 in E (right), F (right); ×2500 in G.

Phenotypic Analysis of the TRPV5$^{-/-}$/ATP6v1b1$^{-/-}$ Mice

TRPV5$^{-/-}$/Atp6v1b1$^{-/-}$ mice were retarded in their growth directly after birth, compared with littermate mice (Figure 2A).

At 5 wk of age, TRPV5$^{-/-}$/Atp6v1b1$^{-/-}$ mice were easily identified because of severe growth retardation (Figure 2B). Moreover, 80% of the TRPV5$^{-/-}$/Atp6v1b1$^{-/-}$ mice died within 6 wk after birth (Figure 2C). These double-knockout mice showed bilateral hydronephrosis (Figure 2D) and abnormal dilation of the CD (Figure 2E). Von Kossa staining in kidneys of 1-wk-old TRPV5$^{-/-}$/Atp6v1b1$^{-/-}$ mice showed massive tubular Ca^{2+} precipitations in the medullary CD (Figure 2, F and G). Subsequently, kidney samples that included the observed precipitates were analyzed by energy-dispersive x-ray microanalysis using a Jeol 1200/STEM (Jeol Ltd., Tokyo, Japan) in combination with a Thermo Noran microanalysis SIX system (Thermo Fisher Scientific Inc., Waltham, MA) (Figure 2H). The x-ray maps and spectrum unequivocally showed the presence of Ca^{2+} and phosphorus (Figure 2, H, 2 and 3, and I) in the precipitates present in the lumen of the CD suggesting Ca^{2+}-phosphate crystals.

Renal and Intestinal Expression of Water, Acid, and Phosphate Transporters

To address renal AQP2 expression levels in control and TRPV5$^{-/-}$ mice, we performed immunoblot analyses. AQP2 was significantly downregulated in TRPV5$^{-/-}$ mice compared with control mice at 8 wk of age (Figure 3A). Moreover, a further AQP2 downregulation was detected in TRPV5$^{-/-}$/Atp6v1b1$^{-/-}$ mice compared with TRPV5$^{-/-}$ mice, analyzed at 5 wk of age (Figure 3B). Membrane fractions were isolated from renal medulla tissue of 8-wk-old TRPV5$^{-/-}$ and control mice. Analysis of AQP2 protein expression in the membrane fractions revealed a significant downregulation in kidneys of TRPV5$^{-/-}$ compared with control littermate mice (Figure 3C). Immunoblotting for the B1 subunit of H^+-ATPase revealed no differences in expression levels between TRPV5$^{-/-}$ and control mice (Figure 4A). Furthermore, a significant downregulation of the renal type IIa NaPi co-transporter (NaPi-IIa) was revealed in TRPV5$^{-/-}$ mice (Figure 4B). In contrast, expression of the intestinal type IIb NaPi co-transporter (NaPi-IIb) was increased in brush border membrane vesicles isolated from ileum of TRPV5$^{-/-}$ mice compared with control mice (Figure 4C).

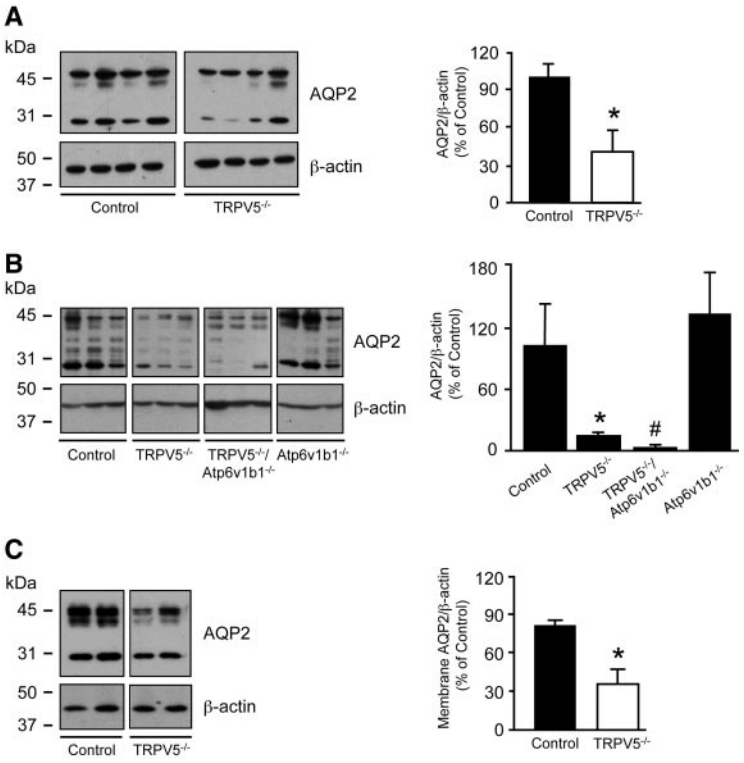

Figure 3. Immunoblotting of renal AQP2. (A) Representative immunoblots for AQP2, revealing 29- and 35- to 50-kD bands representing nonglycosylated and glycosylated AQP2, respectively, which were all included in the semiquantitative determination of renal AQP2 protein abundance from 8-wk-old control *versus* TRPV5$^{-/-}$ mice ($n = 4$). (B) Renal AQP2 protein abundance comparing 5-wk-old control, TRPV5$^{-/-}$, TRPV5$^{-/-}$/Atp6v1b1$^{-/-}$, and Atp6v1b1$^{-/-}$ mice ($n = 3$). (C) AQP2 expression levels in renal medullary membrane fractions from control and TRPV5$^{-/-}$ mice. Broad-range protein and prestained marker bands are depicted, indicating protein size. Expression levels were corrected for β-actin expression. Data were calculated as integrated optical density (arbitrary units), were depicted as percentage of control mice, were presented as means ± SEM, and represented two separate experiments with a total of $n = 4$. $^*P < 0.05$ (significant difference from control); $^{\#}P < 0.05$ (significant difference from TRPV5$^{-/-}$).

Effect of Ca^{2+} on H^+-ATPase Activity of Outer Medullary CDs

We enzymatically isolated outer medullary CDs (OMCDs) from mouse renal tissue to perform pH_i measurements. The activity of H^+-ATPase was determined from the pH_i recovery rate (ΔpH_i/min) after intracellular acidification by NH_4Cl.[25] We investigated the effect on H^+-ATPase activity of low (0.1 mM), normal (1.0 mM), and high (5.0 mM, mimicking the hypercalciuric state of TRPV5$^{-/-}$ mice) extracellular [Ca^{2+}]. Representative recordings are depicted in Figure 5, A and C. Exposure of OMCDs to 5.0 mM [Ca^{2+}] significantly increased H^+-ATPase–mediated pH_i recovery rates in control ($n = 178$ cells; 15 OMCDs; five mice; Figure 5B) and TRPV5$^{-/-}$ mice ($n = 124$ cells; nine OMCDs; four mice; Figure 5D) compared with OMCDs exposed to 0.1 mM [Ca^{2+}] from control mice ($n = 159$ cells; 12 OMCDs; four mice) and TRPV5$^{-/-}$ mice ($n = 149$ cells; 13 OMCDs; five mice). Comparison of pH_i recovery rates in control and TRPV5$^{-/-}$ mouse OMCDs exposed to 0.1 mM [Ca^{2+}] revealed no significant differences in H^+-ATPase activity (Figure 5, B and D). To confirm the specific involvement of the H^+-ATPase proton pump, we performed the following experiments. First, OMCDs were incubated with 100 nM concanamycin, a specific H^+-ATPase inhibitor, which prevented the stimulatory action of 5.0 mM [Ca^{2+}] on the pH_i recovery rate in OMCDs of control as well as

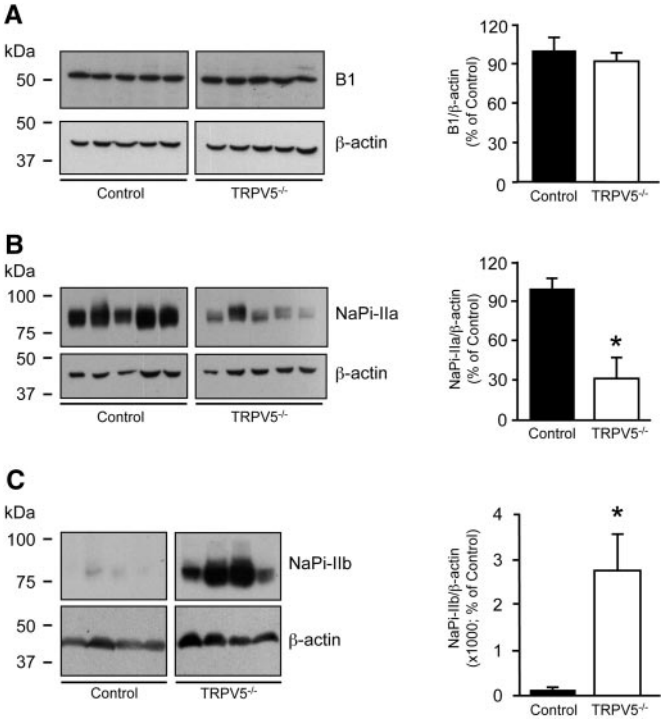

Figure 4. Renal H^+-ATPase B1 subunit, NaPi-IIa co-transporter, and NaPi-IIb co-transporter protein expression. (A) Representative immunoblots for H^+-ATPase B1 subunit (B1), revealing a 56-kD band in total kidney protein lysates of control and TRPV5$^{-/-}$ mice ($n = 5$). (B and C) Representative immunoblots for NaPi-IIa, revealing an approximately 80-kD band in renal cortex ($n = 5$; B), and NaPi-IIb, revealing an approximately 80-kD band in brush border membrane vesicles isolated from total ileum of control and TRPV5$^{-/-}$ mice ($n = 4$; C). Expression levels were normalized for β-actin expression. Broad-range protein marker bands are depicted. Data were calculated as integrated optical density (arbitrary units), depicted as percentage of control mice, and presented as mean ± SEM. *$P < 0.05$ (significant difference from control).

TRPV5$^{-/-}$ mice. Second, the pH_i recovery rates were not affected by 5.0 mM compared with 0.1 mM [Ca^{2+}] in OMCDs of Atp6v1b1$^{-/-}$ mice, underlining an essential role of H^+-ATPase in this acidification process (Figure 5E). OMCDs from control mice were exposed to the CaSR agonist neomycin (200 μM) during the measurements to investigate the molecular mechanism of this Ca^{2+}-mediated increase of H^+-ATPase activity. Neomycin induced a significant increase in the pH_i recovery rate ($n = 100$ cells; eight OMCDs; four mice) compared with nonexposed OMCDs in the presence of 1.0 mM [Ca^{2+}] ($n = 90$ cells; nine OMCDs; four mice), indicating the involvement of CaSR activation (Figure 5F).

DISCUSSION

As illustrated in this study, activation of the CaSR by increased urinary Ca^{2+} levels triggers urinary acidification and polyuria that are crucial adaptations in the prevention of renal stone formation during hypercalciuria. This conclusion is based on the following observations. First, TRPV5$^{-/-}$ mice display hypercalciuria as a result of impaired active Ca^{2+} reabsorption, concomitant hyperphosphaturia, polyuria, and increased urinary acidification, whereas renal Ca^{2+} precipitations are not detected. Second, additional gene ablation of Atp6v1b1 in TRPV5$^{-/-}$ mice prevents the increased urinary acidification and evokes massive Ca^{2+}-phosphate precipitation. Third, activation of the renal CaSR by elevated luminal Ca^{2+} levels stimulates H^+-ATPase–mediated H^+ excretion and renal AQP2 protein downregulation, responsible for the consistent increased urinary acidification and polyuria, respectively, in hypercalciuric TRPV5$^{-/-}$ mice.

Fine-tuning of renal acid excretion is generally accomplished in the CD, where the H^+-ATPase proton pump is localized at the apical side of type A ICs. Exposure to a 5.0 mM Ca^{2+} concentration significantly enhanced H^+-ATPase activity in OMCDs, a specific stimulatory effect that was absent in OMCDs from Atp6v1b1$^{-/-}$ mice. Also, the CaSR agonist neomycin increased H^+-ATPase activity, emphasizing that CaSR activation modulates urinary acid excretion. In TRPV5$^{-/-}$ mice, an increased luminal Ca^{2+} concentration is consistently present in the renal DCT, CNT, and CD.[8] This could activate the apical CaSR, increasing H^+-ATPase activity and thereby initiating the observed acidic urinary pH. Importantly, genetic ablation of TRPV5 increased NAE, which is attributed to a significant rise in urinary TA as a result of hyperphosphaturia. In this perspective, the hyperphosphaturia observed in TRPV5$^{-/-}$ mice could potentially present an acid load to the animals, initially caused by an increase in NaPi-IIb–mediated phosphate absorption; however, previous investigations showed that phosphate administration in healthy volunteers evokes metabolic alkalosis with a concomitant increase of urinary pH and remarkably only transient increases of TA and NAE.[26] Although a higher dietary acid load cannot be completely ruled out, it did not cause a significant change in the acid-base homeostasis of the TRPV5$^{-/-}$ mice. A mild metabolic acidosis would also have increased urinary ammonium excretion, which was not observed; therefore, the decline of the urinary pH in TRPV5$^{-/-}$ mice represents a significant renal acid loss in the presence of hyperphosphaturia. Previously, Nijenhuis *et al.*[27] showed that TRPV5$^{-/-}$ mice display normal blood pH and HCO_3^- levels under basal conditions. These mice become even more alkalemic than wild-type mice when given an $NaHCO_3$ diet *via* the drinking water, which indicates that TRPV5$^{-/-}$ mice do not have a metabolic acidosis. Together with these observations, our data demonstrate that TRPV5$^{-/-}$ mice have increased urinary acidification without an altered systemic acid-base status.

Additional gene ablation of Atp6v1b1 in TRPV5$^{-/-}$ mice normalized urinary pH and caused tubular precipitation of Ca^{2+}-phosphate in the medullary CD. These observations in-

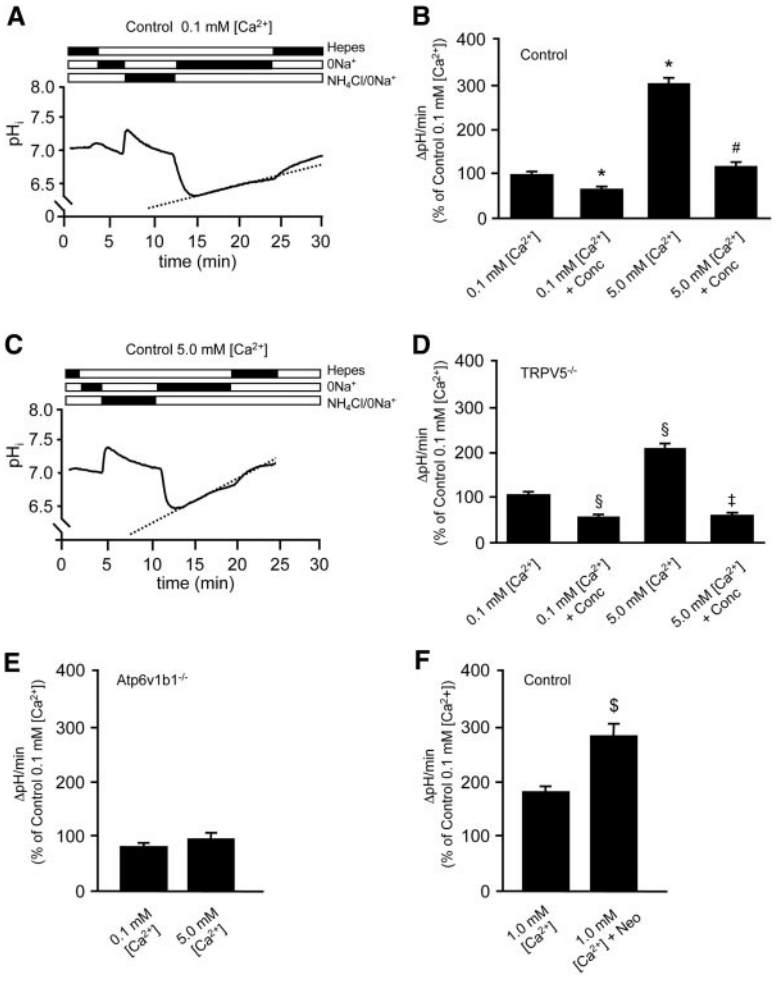

Figure 5. Effect of Ca^{2+} and neomycin on vacuolar H^+-ATPase activity. (A and C) Original pH_i traces from control mouse single OMCD ICs exposed to low (0.1 mM) and high (5.0 mM) [Ca^{2+}], respectively. Bars indicate the alternating HEPES, Na^+-free HEPES, and NH_4Cl-containing buffers applied to the cells. (B and D) Summary of the data from the experiments performed in control and TRPV5$^{-/-}$ mouse OMCD ICs, respectively. (E) ATP6v1b1$^{-/-}$ OMCD ICs exposed to a high (5.0 mM) [Ca^{2+}]. (F) Effect of neomycin (200 μM) on H^+-ATPase activity in control mouse OMCD ICs. (B, D, E, and F) pH recovery rates (ΔpH/min), which are presented as means ± SEM, calculated from number of individual OMCD ICs. $^*P < 0.05$ (significant difference from control 0.1 mM [Ca^{2+}]); $^{\#}P < 0.05$ (significant difference from control 5.0 mM [Ca^{2+}]); $^{\S}P < 0.05$ (significant difference from TRPV5$^{-/-}$ 0.1 mM [Ca^{2+}]); $^{\ddagger}P < 0.05$ (significant difference from TRPV5$^{-/-}$ 5.0 mM [Ca^{2+}]); $^{\$}P < 0.05$ (significant difference from control 1.0 mM [Ca^{2+}]). Conc, concanamycin (100 nM); Neo, neomycin.

dicate that increased H^+-ATPase–mediated urinary acidification in TRPV5$^{-/-}$ mice protects against renal Ca^{2+}-phosphate stone formation. Because the formation of alkaline urine adds to the risk for urinary Ca^{2+}-phosphate precipitation,[28,29] renal stones do occur in patients with distal renal tubular acidosis, who display a urinary acidification defect and hypercalciuria.[15] In accordance with our findings, previous studies demonstrated that extracellular Ca^{2+} levels modulate gastric acid secretion, generally controlled by H^+-K^+-ATPase.[11,30–33] CaSR activation enhanced H^+-K^+-ATPase activity in isolated parietal cells of gastric glands, allowing maximal ionization of dietary Ca^{2+} and establishing enhanced Ca^{2+} absorption from the intestine.[30–33] Furthermore, Farajov *et al.*[34] showed that the activation of the CaSR at the basolateral membrane of medullary TAL cells causes increased acid secretion in a hypercalcemic state. Together with our data, this strongly suggests a key role of the CaSR in linking Ca^{2+} metabolism and acid secretion.

Polyuria can diminish the risk for renal stone formation by reducing the urinary Ca^{2+} concentration. In mice, calciuresis linearly correlated with urinary volume, because an increase of Ca^{2+} excretion leads to an enhanced urinary volume. The consistent polyuria in hypercalciuric TRPV5$^{-/-}$ mice, assessed by a substantial decrease in urinary osmolality, was caused by downregulation of renal AQP2 water channels. Specifically, immunoblot analysis revealed a significant downregulation of AQP2 protein expression levels in isolated renal medullary membrane fractions from TRPV5$^{-/-}$ compared with control mice. Importantly, this is in line with previous studies performed on humans and rats that suggested that activation of the apical CaSR reduces the CD water permeability when the luminal Ca^{2+} level rises.[21,23,35] This involves the CaSR-mediated retrieval of AQP2 from the apical membrane into endocytic compartments. Recently, Bustamante *et al.*[36] showed an attenuated AQP2 expression in a mouse CD cell line after exposure to extracellular Ca^{2+}, neomycin, or Gd^{3+}. Thus, hypercalciuria activates the apical CaSR in the CD and reduces AQP2-mediated water reabsorption, permitting the disposal of excess urinary Ca^{2+} and preventing the formation of stones.

The B1 subunit of the renal H^+-ATPase proton pump, encoded by the Atp6v1b1 gene, is important for urinary acidification in the renal CD.[37,38] Atp6v1b1$^{-/-}$ mice demonstrated hypocalciuria, which is an important difference in phenotype between mice and humans with a genetic Atp6v1b1 defect, although it confirms previous observations of Finberg *et al.*[38] The presence of hypocalciuria in Atp6v1b1$^{-/-}$ has not been explained yet and needs further investigation. Moreover, Atp6v1b1$^{-/-}$ mice displayed a higher urinary pH compared with control mice.[38] Consequently, gene ablation of the Atp6v1b1 gene in TRPV5$^{-/-}$ mice normalized urinary pH. Interestingly, TRPV5$^{-/-}$/Atp6v1b1$^{-/-}$ mice evoked a more severe polyuria than displayed by the TRPV5$^{-/-}$ mice. To explain the increased urinary volume in TRPV5$^{-/-}$/Atp6v1b1$^{-/-}$ mice, the CaSR response as a function of the extracellular pH was previously investigated, showing the functional modulation of the CaSR by extracellular pH.[39,40] The increased urinary

volume in TRPV5$^{-/-}$/Atp6v1b1$^{-/-}$ mice compared with TRPV5$^{-/-}$ mice was explained by a further AQP2 downregulation, demonstrated by immunoblotting. We postulate that the extended decrease of AQP2 expression in the TRPV5$^{-/-}$/Atp6v1b1$^{-/-}$ mice is evoked by the higher sensitivity for Ca^{2+} of the CaSR at a neutral urinary pH. On the basis of previous studies, we conclude that, in the absence of increased urinary acidification in TRPV5$^{-/-}$ mice, a more severe reduction in water reabsorption is induced in an attempt to prevent renal stone formation. Stehberger *et al.*[41] demonstrated a decreased urinary osmolality in AE1-deficient (AE1$^{-/-}$) mice as a result of the retrieval of AQP2 water channels to intracellular vesicles in CD cells. This effect could be the result of increased pH sensitivity of the CaSR at an alkaline environment. Despite the severe polyuria, TRPV5$^{-/-}$/Atp6v1b1$^{-/-}$ mice developed renal Ca^{2+}-phosphate precipitations that obstructed the CD system at an early age. Thus, these results underscore the crucial importance of increased urinary acidification in the local prevention of renal Ca^{2+}-phosphate stones.

TRPV5$^{-/-}$ mice also displayed, besides the hypercalciuria, a profound hyperphosphaturia, increasing the risk for Ca^{2+}-phosphate precipitation. For maintaining normocalcemia, TRPV5$^{-/-}$ mice present with a hypervitaminosis D. Previous investigations showed that increased circulating 1,25-dihydroxyvitamin D_3 levels caused compensatory Ca^{2+} hyperabsorption by upregulation of intestinal Ca^{2+} transporters.[8,42] Moreover, 1,25-dihydroxyvitamin D_3 is an important key player in phosphate homeostasis,[43–45] increasing the abundance of intestinal NaPi-IIb transporters.[46] TRPV5$^{-/-}$ mice displayed a significant upregulation of NaPi-IIb proteins in the ileum, which might evoke phosphate hyperabsorption. Here, we postulate that downregulation of renal NaPi-IIa proteins results in hyperphosphaturia in TRPV5$^{-/-}$ mice, possibly as a compensatory response to the increased phosphate absorption. Whether the NaPi-IIa downregulation could also be an effect of the hypervitaminosis D needs further investigation.

TRPV5$^{-/-}$/Atp6v1b1$^{-/-}$ mice exhibited growth retardation and died before 6 wk of age. The lethal phenotype is likely to be affected by the hydronephrosis, which could be explained by the premature formation of renal stones that physically obstruct the urine flow. This resembles the occurrence of hydronephrosis in congenital nephropathy that is often caused by a functional obstruction in the renal pelvis.[47] Another explanation could be that the hydronephrosis arises in response to the pressure produced by the severe polyuria, dilating the CD and leading to kidney damage. This might also clarify the individual differences in severity of the hydronephrosis, polyuria, and early age of death observed in TRPV5$^{-/-}$/Atp6v1b1$^{-/-}$ mice. A similar observation was previously made in the NKCC2 knockout mice, a mouse model of Bartter syndrome that displayed polyuria and concomitant hydronephrosis as well.[48] Li *et al.*[49] previously investigated the presence of uremia subsequent to urinary tract obstruction in rats, which might have occurred in the TRPV5$^{-/-}$/Atp6v1b1$^{-/-}$ mice as well. The less robust hypercalciuria observed in the TRPV5$^{-/-}$/Atp6v1b1$^{-/-}$ mice in comparison with the single TRPV5$^{-/-}$ mice could be due to the severe increase in urinary volume resulting in a slight dehydration in these mice. This could evoke increased proximal tubular Ca^{2+} reabsorption as a compensatory mechanism, decreasing Ca^{2+} wasting *via* the urine.

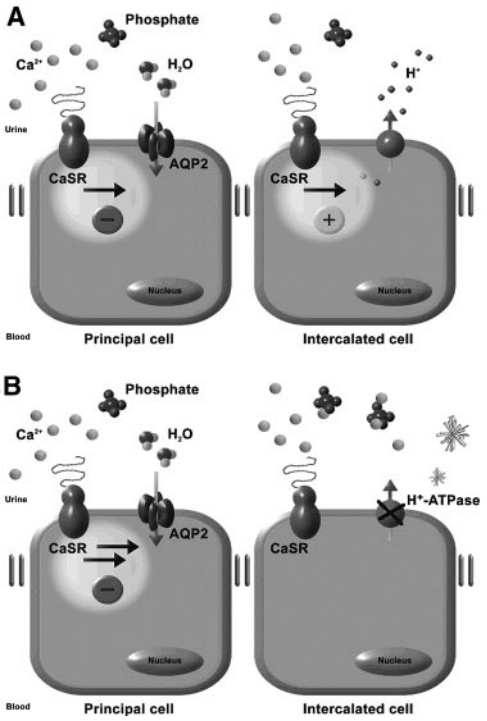

Figure 6. Renal CaSR signaling in the CD. The CaSR is localized at the apical site of principal cells and ICs of the CD. AQP2 proteins are responsible for water reabsorption, whereas H^+-ATPase proteins pump H^+ ions into the urine. (A) In TRPV5$^{-/-}$ mice, the CaSR is activated by increased urinary Ca^{2+} levels. CaSR activation leads to AQP2 downregulation, evoking polyuria. Furthermore, the CaSR triggers urinary acidification by increasing the H^+-ATPase activity. Both polyuria and increased urinary acidification prevent renal Ca^{2+}-phosphate precipitation. (B) Genetic ablation of the Atp6v1b1 gene in the TRPV5$^{-/-}$ mice leads to absence of H^+-ATPase activity and a decrease in urinary acidification. At a urinary pH of 7.4, Ca^{2+}-phosphate precipitates in the CD system of TRPV5$^{-/-}$/Atp6v1b1$^{-/-}$ mice.

In conclusion, the increased urinary acidification and polyuria in response to hypercalciuria are prerequisites to prevent the formation of renal Ca^{2+}-phosphate stones in TRPV5$^{-/-}$ mice. Interestingly, these adaptations involve luminal CaSR activation by increased urinary Ca^{2+} levels, inducing enhanced H^+-ATPase activity and AQP2 downregulation (Figure 6). Renal Ca^{2+}-phosphate stone formers could benefit from the induction of a decrease in urinary pH as well as polyuria that is accomplished by increased water intake. Knowledge of these adaptive mechanisms is relevant for the therapy and prevention of kidney stones.

CONCISE METHODS

Animal Experiments and Metabolic Data

Please see supplemental online information for detailed methods.

Renal Histology

Von Kossa staining of kidney tissue was performed on fixed 5- to 7-μm cryosections to stain Ca^{2+}-containing deposits, and further analysis of renal tubular Ca^{2+} precipitations was performed by transmission electron microscopy. Please see supplemental information for detailed methods.

Protein Isolations and Immunoblotting

To quantify the renal AQP2, the H^+-ATPase B1 subunit, and the NaPi-IIa protein expression levels in 8-wk-old control and TRPV5$^{-/-}$ mice, we prepared renal protein lysates as described before.[42] Membrane fractions were isolated from renal medulla tissue, according to centrifugation methods as described previously.[50,51] For renal AQP2 quantification in the control, TRPV5$^{-/-}$, Atp6v1b1$^{-/-}$, and littermate TRPV5$^{-/-}$/Atp6v1b1$^{-/-}$ mice, kidneys were dissected at 5 wk of age. Ileum brush border membrane vesicles were isolated to quantify NaPi-IIb protein expression levels, as described previously.[43] Blots were incubated with polyclonal antibodies raised in rabbits against AQP2, NaPi-IIa, NaPi-IIb, the B1 subunit of H^+-ATPase, or the monoclonal mouse anti–β-actin antibody. Please see supplemental information for detailed methods.

Tubule Preparations and pH_i Measurements

Mice were transcardially perfused with a digestion buffer containing 1 mg/ml collagenase (Sigma-Aldrich Chemie, Buchs, Switzerland) to obtain renal OMCDs from control, TRPV5$^{-/-}$, and Atp6v1b1$^{-/-}$ mice for H^+-ATPase activity measurements.[25,31,52] BCECF AM (1 μM; Molecular Probes, Invitrogen AG, Basel, Switzerland) was used to monitor pH_i. Cells were acidified using the NH_4Cl (20 mM) prepulse technique, as described previously.[52] Please see supplemental information for detailed methods.

ACKNOWLEDGMENTS

This work was supported by the European Science Foundation (EURYI), the Swiss National Research Foundation (31-109677/1), the EU 6th Framework project EuReGene, the ERA-EDTA, and the Dutch Kidney Foundation (C03.6017).

We thank Drs. R.P. Lifton and K.E. Finberg (Yale University School of Medicine, New Haven, CT) for providing the Atp6v1b1 knockout mice. We also to acknowledge the animal facility of the Radboud University Nijmegen for technical assistance, as well as Drs. L.A. Monnens, J.J. Weening, and C.E. van der Zee for stimulating discussions and technical assistance.

DISCLOSURES

None.

REFERENCES

1. Lerolle N, Lantz B, Paillard F, Gattegno B, Flahault A, Ronco P, Houillier P, Rondeay E: Risk factors for nephrolithiasis in patients with familial idiopathic hypercalciuria. *Am J Med* 113: 99–103, 2002
2. Clark JY, Thompson IM, Optenberg SA: Economic impact of urolithiasis in the United States. *J Urol* 154: 2020–2024, 1995
3. Moe OW, Bonny O: Genetic hypercalciuria. *J Am Soc Nephrol* 16: 729–745, 2005
4. Pak CY, Britton F, Peterson R, Ward D, Northcutt C, Breslau NA, McGuire J, Sakhaee K, Bush S, Nicar M, Norman DA, Peters P: Ambulatory evaluation of nephrolithiasis: Classification, clinical presentation and diagnostic criteria. *Am J Med* 69: 19–30, 1980
5. Sakhaee K, Nicar MJ, Brater DC, Pak CY: Exaggerated natriuretic and calciuric responses to hydrochlorothiazide in renal hypercalciuria but not in absorptive hypercalciuria. *J Clin Endocrinol Metab* 61: 825–829, 1985
6. Frick KK, Bushinsky DA: Molecular mechanisms of primary hypercalciuria. *J Am Soc Nephrol* 14: 1082–1095, 2003
7. Hoenderop JG, Nilius B, Bindels RJ: Calcium absorption across epithelia. *Physiol Rev* 85: 373–422, 2005
8. Hoenderop JG, van Leeuwen JP, van der Eerden BC, Kersten FF, van der Kemp AW, Merillat AM, Waarsing JH, Rossier BC, Vallon V, Hummler E, Bindels RJ: Renal Ca2+ wasting, hyperabsorption, and reduced bone thickness in mice lacking TRPV5. *J Clin Invest* 112: 1906–1914, 2003
9. Wagner CA, Kovacikova J, Stehberger PA, Winter C, Benabbas C, Mohebbi N: Renal Acid-base transport: Old and new players. *Nephron Physiol* 103: 1–6, 2006
10. Kovacikova J, Winter C, Loffing-Cueni D, Loffing J, Finberg KE, Lifton RP, Hummler E, Rossier B, Wagner CA: The connecting tubule is the main site of the furosemide-induced urinary acidification by the vacuolar H+-ATPase. *Kidney Int* 70: 1706–1716, 2006
11. Wagner CA, Finberg KE, Breton S, Marshansky V, Brown D, Geibel JP: Renal vacuolar H+-ATPase. *Physiol Rev* 84: 1263–1314, 2004
12. Karet FE, Finberg KE, Nelson RD, Nayir A, Mocan H, Sanjad SA, Rodriguez-Soriano J, Santos F, Cremers CW, Di Pietro A, Hoffbrand BI, Winiarski J, Bakkaloglu A, Ozen S, Dusunsel R, Goodyer P, Hulton SA, Wu DK, Skvorak AB, Morton CC, Cunningham MJ, Jha V, Lifton RP: Mutations in the gene encoding B1 subunit of H+-ATPase cause renal tubular acidosis with sensorineural deafness. *Nat Genet* 21: 84–90, 1999
13. Karet FE, Finberg KE, Nayir A, Bakkaloglu A, Ozen S, Hulton SA, Sanjad SA, Al-Sabban EA, Medina JF, Lifton RP: Localization of a gene for autosomal recessive distal renal tubular acidosis with normal hearing (rdRTA2) to 7q33–34. *Am J Hum Genet* 65: 1656–1665, 1999
14. Unwin RJ, Shirley DG, Capasso G: Urinary acidification and distal renal tubular acidosis. *J Nephrol* 15[Suppl 5]: S142–S150, 2002
15. Buckalew VM Jr: Nephrolithiasis in renal tubular acidosis. *J Urol* 141: 731–737, 1998
16. Sayer JA, Carr G, Simmons NL: Nephrocalcinosis: Molecular insights into calcium precipitation within the kidney. *Clin Sci (Lond)* 106: 549–561, 2004
17. Tessitore N, Ortalda V, Fabris A, D'Angelo A, Rugiu C, Oldrizzi L, Lupo A, Valvo E, Gammaro L, Loschiavo C: Renal acidification defects in patients with recurrent calcium nephrolithiasis. *Nephron* 41: 325–332, 1985
18. Gault MH, Chafe LL, Morgan JM, Parfrey PS, Harnett JD, Walsh EA, Prabhakaran VM, Dow D, Colpitts A: Comparison of patients with idiopathic calcium phosphate and calcium oxalate stones. *Medicine* 70: 345–359, 1991
19. van Os CH, Deen PM: Role of aquaporins in renal water handling: Physiology and pathophysiology. *Nephrol Dial Transplant* 13: 1645–1651, 1998
20. Deen PM, Verdijk MA, Knoers NV, Wieringa B, Monnens LA, van Os CH, van Oost BA: Requirement of human renal water channel aquaporin-2 for vasopressin-dependent concentration of urine. *Science* 264: 92–95, 1994

21. Earm JH, Christensen BM, Frokiaer J, Marples D, Han JS, Knepper MA, Nielsen S: Decreased aquaporin-2 expression and apical plasma membrane delivery in kidney collecting ducts of polyuric hypercalcemic rats. *J Am Soc Nephrol* 9: 2181–2193, 1998
22. Sands JM, Flores FX, Kato A, Baum MA, Brown EM, Ward DT, Hebert SC, Harris HW: Vasopressin-elicited water and urea permeabilities are altered in IMCD in hypercalcemic rats. *Am J Physiol* 274: F978–F985, 1998
23. Sands JM, Naruse M, Baum M, Jo I, Hebert SC, Brown EM, Harris HW: Apical extracellular calcium/polyvalent cation-sensing receptor regulates vasopressin-elicited water permeability in rat kidney inner medullary collecting duct. *J Clin Invest* 99: 1399–1405, 1997
24. Riccardi D, Hall AE, Chattopadhyay N, Xu JZ, Brown EM, Hebert SC: Localization of the extracellular Ca2+/polyvalent cation-sensing protein in rat kidney. *Am J Physiol* 274: F611–F622, 1998
25. Wagner CA, Lukewille U, Valles P, Breton S, Brown D, Giebisch GH, Geibel JP: A rapid enzymatic method for the isolation of defined kidney tubule fragments from mouse. *Pflugers Arch* 446: 623–632, 2003
26. Krapf R, Glatz M, Hulter HN: Neutral phosphate administration generates and maintains renal metabolic alkalosis and hyperparathyroidism. *Am J Physiol* 268: F802–F807, 1995
27. Nijenhuis T, Renkema KY, Hoenderop JG, Bindels RJ: Acid-base status determines the renal expression of Ca2+ and Mg2+ transport proteins. *J Am Soc Nephrol* 17: 617–626, 2006
28. Darn SM, Sodi R, Ranganath LR, Roberts NB, Duffield JR: Experimental and computer modelling speciation studies of the effect of pH and phosphate on the precipitation of calcium and magnesium salts in urine. *Clin Chem Lab Med* 44: 185–191, 2006
29. Ackermann D, Baumann JM: Chemical factors governing the state of saturation towards brushite and whewellite in urine of calcium stone formers. *Urol Res* 15: 63–65, 1987
30. Geibel JP, Wagner CA, Caroppo R, Qureshi I, Gloeckner J, Manuelidis L, Kirchhoff P, Radebold K: The stomach divalent ion-sensing receptor scar is a modulator of gastric acid secretion. *J Biol Chem* 276: 39549–39552, 2001
31. Dufner MM, Kirchhoff P, Remy C, Hafner P, Muller MK, Cheng SX, Tang LQ, Hebert SC, Geibel JP, Wagner CA: The calcium-sensing receptor acts as a modulator of gastric acid secretion in freshly isolated human gastric glands. *Am J Physiol Gastrointest Liver Physiol* 289: G1084–G1090, 2005
32. Remy C, Kirchhoff P, Hafner P, Busque SM, Mueller MK, Geibel JP, Wagner CA: Stimulatory pathways of the calcium-sensing receptor on acid secretion in freshly isolated human gastric glands. *Cell Physiol Biochem* 19: 33–42, 2007
33. Kirchhoff P, Geibel JP: Role of calcium and other trace elements in the gastrointestinal physiology. *World J Gastroenterol* 12: 3229–3236, 2006
34. Farajov EI, Morimoto T, Aslanova UF, Kumagai N, Sugawara N, Kondo Y: Calcium-sensing receptor stimulates K+-dependent H+ excretion in medullary thick ascending limbs of Henle's loop of mouse kidney. *Tohoku J Exp Med* 216: 7–15, 2008
35. Gill JR Jr, Bartter FC: On the impairment of renal concentrating ability in prolonged hypercalcemia and hypercalciuria in man. *J Clin Invest* 40: 716–722, 1961
36. Bustamante M, Hasler U, Leroy V, de Seigneux S, Dimitrov M, Mordasini D, Rousselot M, Martin PY, Féraille E: Calcium-sensing receptor attenuates AVP-induced aquaporin-2 expression via a calmodulin-dependent mechanism. *J Am Soc Nephrol* 19: 109–116, 2008
37. Schwartz JH, Li G, Yang Q, Suri V, Ross JJ, Alexander EA: Role of SNAREs and H+-ATPase in the targeting of proton pump-coated vesicles to collecting duct cell apical membrane. *Kidney Int* 72: 1310–1315, 2007
38. Finberg KE, Wagner CA, Bailey MA, Paunescu TG, Breton S, Brown D, Giebisch G, Geibel JP, Lifton RP: The B1-subunit of the H+-ATPase is required for maximal urinary acidification. *Proc Natl Acad Sci U S A* 102: 13616–13621, 2005
39. Quinn SJ, Bai M, Brown EM: pH Sensing by the calcium-sensing receptor. *J Biol Chem* 279: 37241–37249, 2004
40. Doroszewicz J, Waldegger P, Jeck N, Seyberth H, Waldegger S: pH dependence of extracellular calcium sensing receptor activity determined by a novel technique. *Kidney Int* 67: 187–192, 2005
41. Stehberger PA, Shmukler BE, Stuart-Tilley AK, Peters LL, Alper SL, Wagner CA: Distal renal tubular acidosis in mice lacking the AE1 (band3) Cl−/HCO3− exchanger (slc4a1). *J Am Soc Nephrol* 18: 1408–1418, 2007
42. Renkema KY, Nijenhuis T, van der Eerden BC, van der Kemp AW, Weinans H, van Leeuwen JP, Bindels RJ, Hoenderop JG: Hypervitaminosis D mediates compensatory Ca2+ hyperabsorption in TRPV5 knockout mice. *J Am Soc Nephrol* 16: 3188–3195, 2005
43. Radanovic T, Wagner CA, Murer H, Biber J: Regulation of intestinal phosphate transport: I. Segmental expression and adaptation to low-Pi diet of the type IIb Na+-Pi cotransporter in mouse small intestine. *Am J Physiol Gastrointest Liver Physiol* 288: G496–G500, 2005
44. Cross HS, Debiec H, Peterlik M: Mechanism and regulation of intestinal phosphate absorption. *Miner Electrolyte Metab* 16: 115–124, 1990
45. Xu H, Bai L, Collins JF, Ghishan FK: Age-dependent regulation of rat intestinal type IIb sodium-phosphate cotransporter by 1,25-(OH)2 vitamin D3. *Am J Physiol* 282: C487–C493, 2002
46. Capuano P, Radanovic T, Wagner CA, Bacic D, Kato S, Uchiyama Y, St-Arnoud R, Murer H, Biber J: Intestinal and renal adaptation to a low-Pi diet of type II NaPi cotransporters in vitamin D receptor- and 1alphaOHase-deficient mice. *Am J Physiol* 288: C429–C434, 2005
47. Mendelsohn C: Functional obstruction: The renal pelvis rules. *J Clin Invest* 113: 957–959, 2004
48. Takahashi N, Chernavvsky DR, Gomez RA, Igarashi P, Gitelman HJ, Smithies O: Uncompensated polyuria in a mouse model of Bartter's syndrome. *Proc Natl Acad Sci U S A* 97: 5434–5439, 2000
49. Li C, Klein JD, Wang W, Knepper MA, Nielsen S, Sands JM, Frøkiaer J: Altered expression of urea transporters in response to ureteral obstruction. *Am J Physiol Renal Physiol* 286: F1154–F1162, 2004
50. van Baal J, Yu A, Hartog A, Fransen JA, Willems PH, Lytton J, Bindels RJ: Localization and regulation by vitamin D of calcium transport proteins in rabbit cortical collecting system. *Am J Physiol* 271: F985–F993, 1996
51. Shaw S, Marples D: A rat kidney tubule suspension for the study of vasopressin-induced shuttling of AQP2 water channels. *Am J Physiol Renal Physiol* 283: F1160–F1166, 2002
52. Winter C, Schulz N, Giebisch G, Geibel JP, Wagner CA: Nongenomic stimulation of vacuolar H+-ATPases in intercalated renal tubule cells by aldosterone. *Proc Natl Acad Sci U S A* 101: 2636–2641, 2004

See related editorial, "Does Idiopathic Hypercalciuria Trigger Calcium-Sensing Receptor–Mediated Protection from Urinary Supersaturation?" on pages 1657–1659.

Supplemental information for this article is available online at http://www.jasn.org/.